Available online at www.sciencedirect.com
SCIENCE DIRECT
Optics Communications 264 (2006) 45–50
OPTICS COMMUNICATIONS
www.elsevier.com/locate/optcom

Interlacing multiplexing techniques for optical morphological correlation

Zeev Zalevksy [a], Javier García [b], Pascuala García-Martínez [b,*]

[a] School of Engineering, Bar-Ilan University, Ramat-Gan 52900, Israel
[b] Departamento de Óptica, Universitat de València, c/Dr. Moliner, 50, 46100 Burjassot, Valencia, Spain

Received 8 November 2005; received in revised form 2 February 2006; accepted 6 February 2006

Abstract

We propose a novel approach to implement nonlinear morphological correlation. Previous implementation was based on a time sequential approach that consists on displaying different binary image decomposition in a joint transform correlator adding each joint power spectra sequentially. A second Fourier transformation of the sum of joint power spectra gives the correlation output. In this paper, we propose to interlace the different binary images into one single distribution. Then, we introduce the distribution in a conventional joint transform correlator. The correlation output gives the morphological correlation at a specific location. The advantage is important considering that no sequential approach is needed anymore, so the necessary number of correlations is reduced. Optical implementation results are provided.

1. Introduction

Linear correlation for pattern recognition is the most popular operation in optical signal processing [1,2]. Most optical pattern recognition techniques involve either the use of a matched filter based correlator [3] or of a joint transform correlator (JTC) [4,5]. A matched filter based correlator uses Fourier domain complex filter synthesis, whereas a JTC utilizes spatial domain filter synthesis. Linear correlation is associated with low correlation discrimination and large correlation side-lobes and large auto-correlation bandwidth. Moreover, the common matched filter is optimum in the mean square error (MSE) sense, meaning that maximizing the MSE leads to maximizing the common linear correlation (LC) [6]. The MSE is a function of the norm and the acceptance of the LC is due to the mathematical tractability of the square error metric and the simple optical implementation. Another metric is the mean absolute error (MAE). It has been shown that minimizing the MAE criterion is equivalent to maximizing a nonlinear correlation namely the morphological correlation (MC) [7]. The MC presents higher discrimination capability for pattern recognition as compared with common LC. Also, due to its nonlinearity property, MC offers a more robust detection of low-intensity images in the presence of high-intensity patterns which are to be rejected. Because of that MC has been shown to be an important tool for optical pattern recognition [8–13]. MC is defined by means of linear correlations between binary decompositions of the input scene and the reference. Moreover, MC can be implemented optically with a JTC. The main drawback of MC is that involves many linear correlations. The number of correlations is connected with the number of gray levels at the image. For common MC definition [7,8] between 256 gray level images, one needs to perform 256 linear correlations. In order to reduce the number of correlations involved in the process, we defined a modification of the MC based on bit-representation decomposition [9], where for previous example ($2^8 = 256$), only eight linear correlations are required. Indeed, this process reduces the number of correlation, but still remains the need to sum the results of the correlations.

In order to overcome the implementation of many correlations, in this paper we introduce an interlacing technique

* Corresponding author. Tel./fax: +34 963544717.
E-mail address: pascuala.garcia@uv.es (P. García-Martínez).

0030-4018/$ - see front matter © 2006 Elsevier B.V. All rights reserved.
doi:10.1016/j.optcom.2006.02.011

to codify the binary bit-plane joint input images in a single amplitude distribution. Interlacing techniques have been used widely in optical signal processing basically for computer generated holograms [14,15]. The idea of those papers is to design a number of subholograms in a specific geometrical configuration and add up their reconstructed images coherently to a single desired image. However, those techniques involve an iterative approach to reduce the reconstruction errors. In this paper, we used the interlacing process to encode the different binary images using a certain geometrical configuration. The encoded amplitude distribution is then sent to a JTC. The correlation output distribution produces interlaced cross-correlations between the binary slices. Morphological correlation is obtained for a specific location. We calculate the location for MC and we present both simulated and optical results.

Section 2 provides some mathematical background on morphological correlations. In Section 3, we present the description of the proposed approach. Sections 4 and 5 deal with the numerical and the experimental results, respectively. The manuscript is concluded in Section 6.

2. Morphological correlation

The MC was described in Refs. [7,8]. Nevertheless, for completeness, we repeat fundamental expressions in the following.

Let $f(x,y)$ and $g(x,y)$ be the reference and the input scene real valued objects, respectively. The conventional linear correlation between $f(x,y)$ and $g(x,y)$ is

$$\begin{aligned} LC_{fg}(x,y) &= f(x,y) * g(x,y) \\ &= \sum_{u,v} f(u+x, v+y) g(u,v), \end{aligned} \tag{1}$$

where $*$ denotes the correlation symbol.

The morphological correlation is defined as [7]

$$MC_{fg}(x,y) = \sum_{u,v} \min[f(u+x, v+y), g(u,v)], \tag{2}$$

where the minimum operation comes from the minimization of the MAE, whereas the product of the LC (see Eq. (1)) comes from the minimization of the MSE [6].

Latter definitions of MC can be expressed in terms of a thresholding function and linear correlations [7,8] as

$$MC_{fg}(x,y) = \sum_{q=0}^{Q-1} [f_q * g_q](x,y), \tag{3}$$

where Q is the total number of gray levels of images and

$$f_q(x,y) = \begin{cases} 1 & \text{if } f(x,y) \geqslant q, \\ 0 & \text{otherwise,} \end{cases} \quad g_q(x,y) = \begin{cases} 1 & \text{if } g(x,y) \geqslant q, \\ 0 & \text{otherwise} \end{cases} \tag{4}$$

Eq. (3) means that the MC can be defined in terms of a summation of linear correlations between the same q-binary thresholded slices of the reference and the input. The optical correlation of the MC [8] is carried out by means of a JTC scheme [4]. The nonlinearity provides as a bonus the detection of low-intensity images in the presence of high-intensity patterns.

Although Eq. (3) is the common definition of the MC, in this paper we use a binary decomposition based on bit plane representation [9]. So, the reference and the input are decomposed into a set of binary slices, each corresponding to a specific bit in the binary representation of the image. From now on, the definition of modified morphological correlation (MMC) is

$$MMC_{fg}(x,y) = \sum_{q=0}^{N-1} [B_q[f(x,y)]] * [B_q[g(x,y)]], \tag{5}$$

where $B_q[\cdot]$ is the of qth bit plane distribution, and N is the number of bit planes involved in the process. More generally, for $Q = 2^N$ quantization levels, the MMC defined in Eq. (5) requires $N = \log_2 Q$ correlation operations rather than the Q operations in the MC. An additional advantage of the MMC process is that it improves discrimination capabilities and thus yields a more selective system [9].

MMC can be implemented optically: Let $f(x + x_0, y)$ and $g(x - x_0, y)$ be the reference and the input scene objects centered at $(-x_0, 0)$ and $(x_0, 0)$, respectively. Each pair of elementary binary joint input bit slices (one slice from the reference object and one from the input scene) are placed next to each other in the input plane. For each pair, the joint power spectrum is performed. The summation of the joint power spectrum for all the slices is

$$\begin{aligned} JPS_{\Sigma}(u,v) &= \sum_{q=0}^{N-1} JPS_q \\ &= \sum_{q=0}^{N-1} |FT\{B_q[f]\}|^2 + \sum_{q=0}^{N-1} |FT\{B_q[g]\}|^2 \\ &\quad + \sum_{q=0}^{N-1} FT\{B_q[f]\}^* FT\{B_q[g]\} \exp[-\mathrm{i}2\phi_q(u,v)] \\ &\quad + \sum_{q=0}^{N-1} FT\{B_q[f]\} FT\{B_q[g]\}^* \exp[\mathrm{i}2\phi_q(u,v)], \end{aligned} \tag{6}$$

where FT is the Fourier transform and $\phi(u,v) = \frac{2\pi u x_0}{(\lambda f)}$, with f being the focal length of the lens and λ the wavelength of the illumination coherent light. The Fourier transform of the third term of Eq. (6) yields the MMC correlation as

$$\begin{aligned} &FT\left\{ \sum_{q=0}^{N-1} FT\{B_q[f]\}^* FT\{B_q[g]\} \exp[-\mathrm{i}2\phi_q(u,v)] \right\} \\ &= \sum_{q=0}^{N-1} [B_q[f] * B_q[g]](x - 2x_0, y). \end{aligned} \tag{7}$$

In addition the Fourier transform of the fourth term is the conjugate of the MMC correlation.

3. Interlacing techniques for morphological correlation

The proposed improvement of the MMC implementation will be analyzed in this section. Although MMC

reduces significantly the number of the required linear correlations, we proposed to reduce to only one correlation after a codification of the binary bit planes of the reference and of the input using interlacing techniques rather than placing them side by side. We will use an interlacing as shown in Fig. 1 for the binary bit planes of input scene as well as the binary bit planes for the reference object. Note that the different bit planes are represented by different texture patterns in order to illustrate clearly the algorithm. To obtain a final joint interlaced image, we combined the information of the bit maps of image $f(x,y)$ and of $g(x,y)$ as shown in Fig. 2. Note that the period, in pixels, of that distribution is twice the number of bit planes in the decomposition. We will assume vertical interlacing so, we consider 1D signals analysis for simplicity. The interlacing technique can be viewed as a sampling method. Eq. (8) shows the interlacing for the reference image as

$$I_f(x) = \sum_s \left(\left\{ \sum_{k=0}^{N-1} B_k[f(x)]\delta(x - s\Delta x) \right\} \otimes \delta\left(x - \frac{k}{2N}\Delta x \right) \right), \tag{8}$$

where Δx is the size for the joint interlaced gap (see Fig. 2) and N is the number of bit planes for the reference function, $f(x)$. The index s represents a sampling index for the joint interlaced image and the index k represents the sampling inside the interval Δx (running over the bit planes). Moreover, the input scene, $g(x)$, has to be interlaced next to the reference function according to

$$I_g(x) = \sum_s \left(\left\{ \sum_{k=0}^{N-1} B_k[g(x)]\delta(x - s\Delta x) \right\} \otimes \delta\left(x - \frac{(k+N-1)}{2N}\Delta x \right) \right). \tag{9}$$

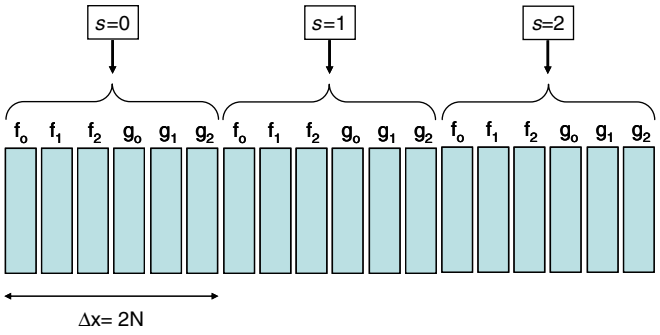

Fig. 2. Interlacing algorithm for joint input JTC image.

Again, the index k represents the sampling inside the interval, Δx, and it permits to interlace the different binary bit planes for $f(x)$ and $g(x)$.

The final joint interlaced image (Fig. 2) can be described as $I(x) = I_f(x) + I_g(x)$.

Let us assume $Q = 8$ gray levels, so that there are $N = 3$ bit planes. Once we codify the information of $f(x,y)$ and $g(x,y)$ as in Fig. 2, we introduce that distribution in a JTC. First, a Fourier transformation is obtained, and after registering the joint power spectrum of the distribution, a second Fourier transformation gives the correlation output. In fact, the correlation output will be a complex distribution with many cross-correlation terms. Due to interlacing techniques, different correlations are obtained just by selecting the appropriated pixels out of the JTC output plane. For the sake of clarity Fig. 3(a) represents the correlation between interlaced patterns at the origin, it means no shift between both patterns. The result is the addition of all auto-correlation terms as it is shown in Fig. 3(a). For the sake of clarity, in Fig. 4 we have drawn the correlation output plane with all the cross-correlation

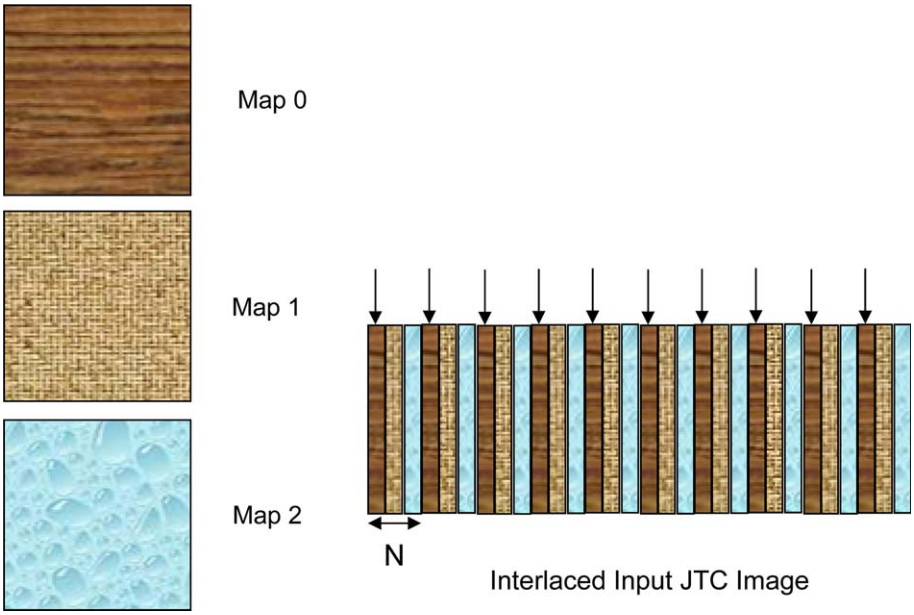

Fig. 1. Interlacing algorithm for images codification.

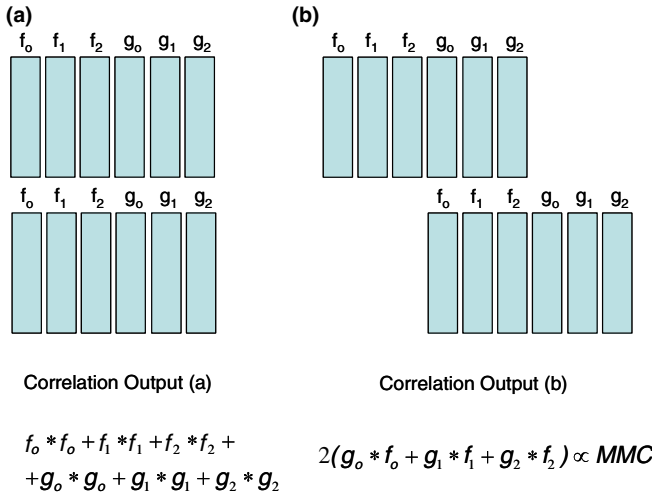

Fig. 3. Relations between interlacing and correlation.

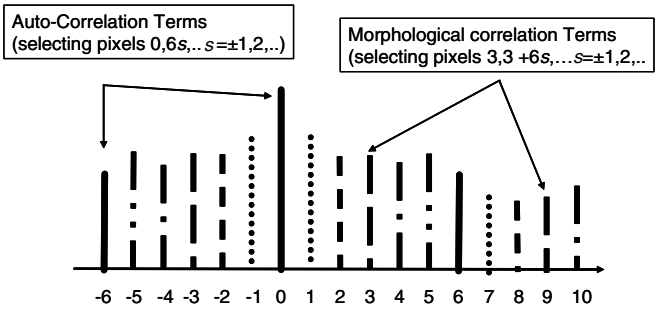

Fig. 4. The cross-section of the output.

terms. In Fig. 4, we show which pixels has to be selected in order to obtain the addition of all auto-correlation terms.

Moreover, if the shift between the interlaced patterns is 3 pixels, then the correlation output coincides with the morphological correlation as it is shown in Fig. 3(b). In Fig. 4, we mark the position of the pixels that have to be selected in order to obtain the MMC.

4. Computer simulations

The input scene is shown in Fig. 5. It consists out of two different cars. The reference car is placed below. The image has eight gray levels, it means that it can be decomposed using three binary bit planes, as shown in Fig. 6. We codify the the bit planes of the input scene (Fig. 5) with three bit planes of the reference car. In order to obtain correlation peaks in a different position from the origin, a small displacement between the targets at the input scene results in a small displacement of the zero-order correlation peak. After the interlacing algorithm (see Fig. 2), we simulate the JTC process. The correlation output with all interlaced cross-correlations is shown in Fig. 7. By selecting the appropriated pixels (see Fig. 4), we can obtain the morphological correlation among other correlations. Fig. 8 represents the MMC correlation. Note that the small

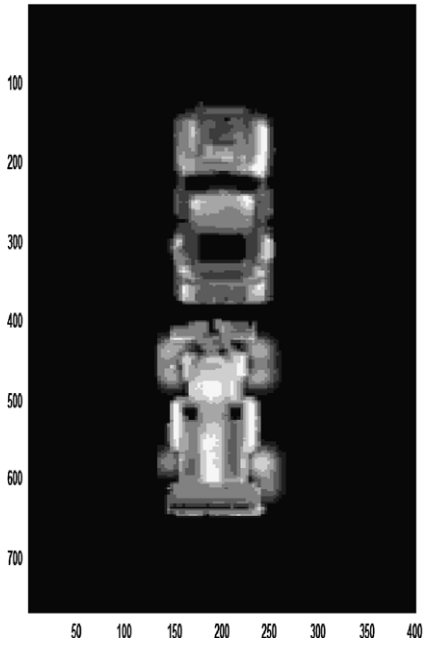

Fig. 5. The gray-level input scene image. The reference object is placed on the lower part.

displacement between the input and the reference results with a shift in the auto-morphological correlation peak. The MMC detects the correct target discriminating properly against the other false target. Note that the size of the interlaced correlation output (Fig. 7) for x-axis is 2400 pixels, whereas for the MMC output (Fig. 8) it is 400 pixels because we are selecting pixels using intervals of 6 pixels.

5. Experimental results

In this section, we have implemented optically the MMC using the interlacing approach with a spatial light modulator (SLM) working in amplitude modulation. The SLM that we use for the optical experiments is a XGA LCTV from CRL Smetic Technology. We have calibrated the panel to work as almost amplitude-only modulator. We have worked with a blue laser ($\lambda = 473$ nm). The corresponding joint power spectrum (JPS) is captured by a CCD camera and then the second Fourier transformation is done optically.

The interlaced image introduced at the modulator may be seen in Fig. 9. The joint power spectrum is shown in Fig. 10. Note the repetition of the spectrum caused because we are sampling the images with an interval of 6 pixels. After that, we introduce the JPS of Fig. 9 into the modulator and a second Fourier transform produced the correlation output plane. Again, selecting the appropriated pixels we got the MMC correlation shown in Fig. 11. Note that the two correlation peaks from the MMC do not have the same energy. This is because the JPS of Fig. 10 is not exactly symmetrical. It can be also because of non-uniform illuminations.

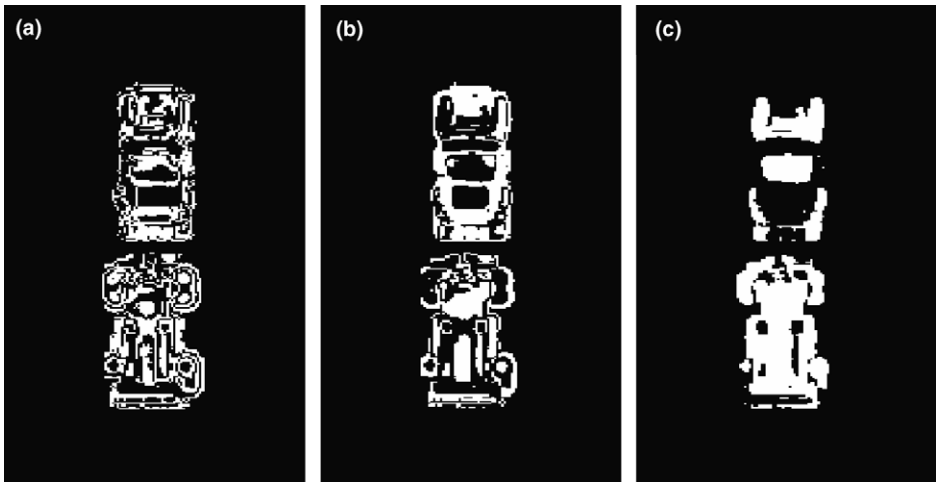

Fig. 6. (a) Bit plane 2. (b) Bit plane 1. (c) Bit plane 0.

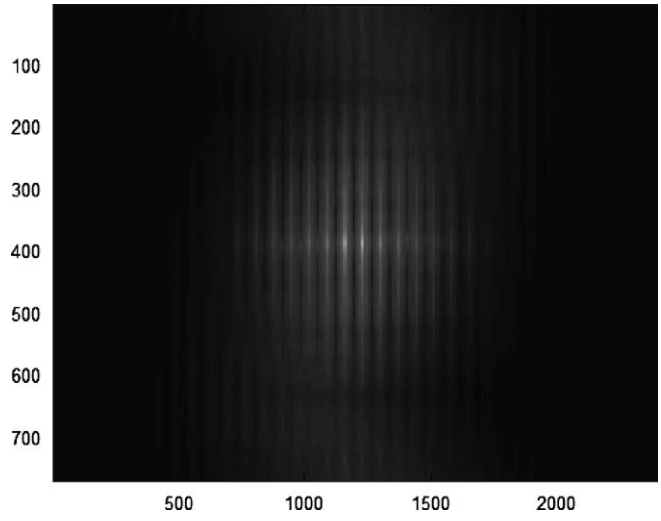

Fig. 7. Interlaced correlation output.

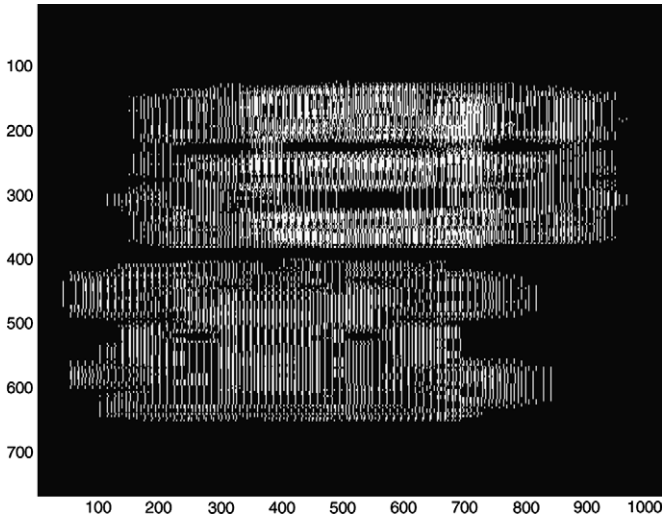

Fig. 9. JTC input image.

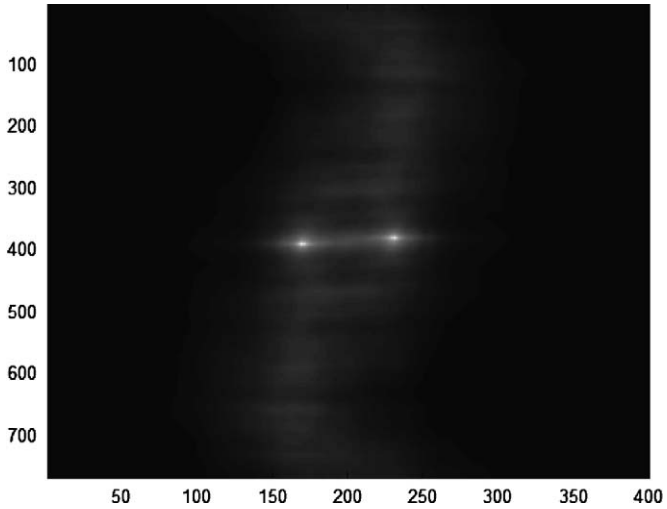

Fig. 8. MMC using interlacing techniques taking every 6th pixel.

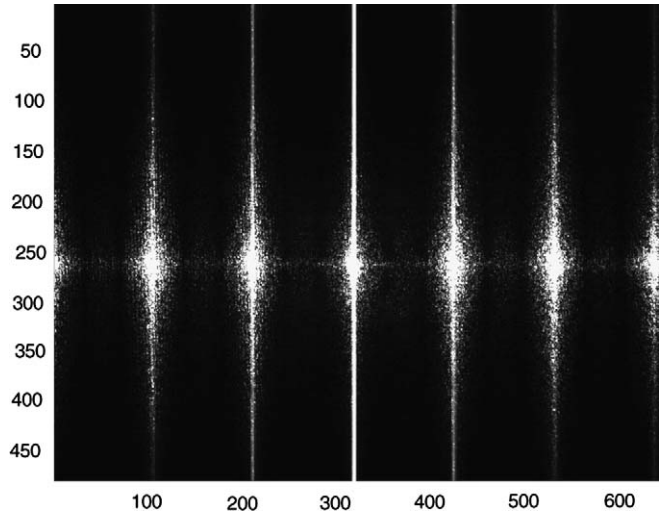

Fig. 10. The joint power spectrum of Fig. 9.

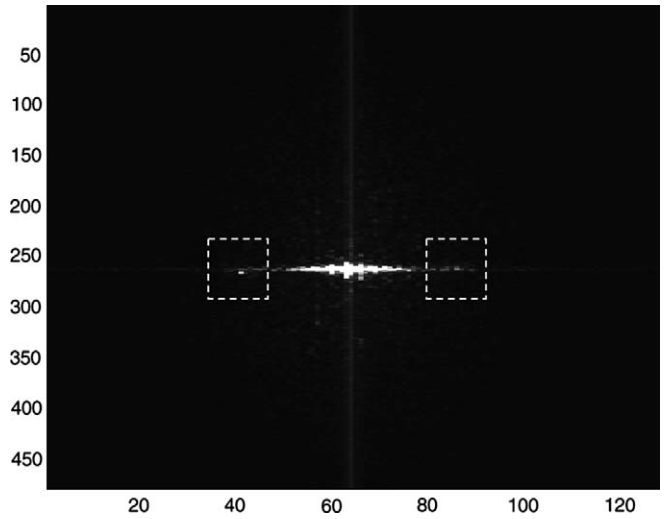

Fig. 11. Experimental MMC with one single step using interlacing techniques. The auto-MMC peaks are marked with a square.

6. Conclusion

This paper has discussed an efficient method to implement morphological correlation with the requirement of only one correlation. Morphological correlations, as well as other nonlinear correlations, are based on summation of linear correlations between binary decomposed images. The method proposed in this paper interlaces different bit planes from the reference and the input scene into one single amplitude distribution. The morphological correlation is obtained for a specific location of the output plane. The higher discrimination ability is maintained as it is shown in the optical experiments.

Acknowledgments

This work was supported by FEDER funds and the Spanish Ministerio de Educación y Ciencia under the project FIS2004-06947-C02-01, the Agencia Valenciana de Ciencia y Tecnología (AVCT), project GRUPOS03/117, the D.G Investigació i Transferència Tecnològica, project IIARC0/2004/217.

References

[1] J.W. Goodman, Introduction to Fourier Optics, second ed., McGraw-Hill, New York, 1996.
[2] B.G. Boone, Signal Processing using Optics: Fundamentals, Devices, Architectures, and Applications, Oxford University Press, Oxford, 1998.
[3] A. VanderLugt, IEEE Trans. Inf. Theory IT-10 (1964) 139.
[4] C.S. Weaver, J.W. Goodman, Appl. Opt. 5 (1966) 1248.
[5] F.T.S. Yu, X.J. Lu, Opt. Commun. 52 (1984) 10.
[6] R.O. Duda, P.E. Hart, Pattern Classification and Scene Analysis, Wiley, New York, 1973, p. 279 (Chapter 7).
[7] P. Maragos, R.W. Schafer, Proc. IEEE 78 (1990) 690.
[8] P. García-Martínez, D. Mas, J. García, C. Ferreira, Appl. Opt. 37 (1998) 2112.
[9] A. Shemer, D. Mendlovic, G. Shabtay, P. García-Martínez, J. García, Appl. Opt. 38 (1999) 781.
[10] P. García-Martínez, C. Ferreira, D. Mendlovic, J. Opt. A 1 (1999) 719.
[11] P. García-Martínez, C. Ferreira, J. García, H.H. Arsenault, Appl. Opt. 39 (2000) 776.
[12] S.Q. Zhang, M.A. Karim, Appl. Opt. 38 (1999) 7228.
[13] A. Fares, P. García-Martínez, C. Ferreira, M. Hamdi, A. Bouzid, Opt. Commun. 203 (2002) 255.
[14] O.K. Ersoy, J.Y. Zhuang, J. Brede, Appl. Opt. 31 (1992) 6894.
[15] S. Yang, T. Shimomura, Appl. Opt. 35 (1996) 6983.